



Review

Unlocking Insights into Folding, Structure, and Function of Proteins through Circular Dichroism Spectroscopy—A Short Review

Leonardo A. Linhares and Carlos H. I. Ramos *

Institute of Chemistry, University of Campinas—UNICAMP, Campinas 13083-970, SP, Brazil

* Correspondence: cramos@iqm.unicamp.br; Tel.: +55-19-3521-3096

Abstract: Circular dichroism (CD) spectroscopy has emerged as a powerful tool in the study of protein folding, structure, and function. This review explores the versatile applications of CD spectroscopy in unraveling the intricate relationship between protein conformation and biological activity. A key advantage of CD spectroscopy is its ability to analyze protein samples with minimal quantity requirements, making it an attractive technique for studying proteins that are scarce or difficult to produce. Moreover, CD spectroscopy enables the monitoring of physical and chemical environmental effects on protein structures, providing valuable insights into the dynamic behavior of proteins in different conditions. In recent years, the use of synchrotron radiation as a light source for CD measurements has gained traction, offering enhanced sensitivity and resolution. By combining the advantages of CD spectroscopy, such as minimal sample requirements and the ability to probe environmental effects, with the emerging capabilities of synchrotron radiation (SRCD), researchers have an unprecedented opportunity to explore the diverse aspects of protein behavior. This review highlights the significance of CD spectroscopy in protein research and the growing role of synchrotron radiation in advancing our understanding of protein behavior, aiming to provide novel insights and applications in various fields, including drug discovery, protein engineering, and biotechnology. A brief overview of Solid-State Circular Dichroism (SSCD) is also included.

Keywords: circular dichroism; protein folding; protein stability; spectroscopy; SRCD



Citation: Linhares, L.A.; Ramos, C.H.I. Unlocking Insights into Folding, Structure, and Function of Proteins through Circular Dichroism Spectroscopy—A Short Review. *Appl. Biosci.* **2023**, *2*, 639–655. <https://doi.org/10.3390/applbiosci2040040>

Academic Editor:
Hervé Quiquampoix

Received: 27 September 2023
Revised: 30 October 2023
Accepted: 21 November 2023
Published: 24 November 2023



Copyright: © 2023 by the authors. Licensee MDPI, Basel, Switzerland. This article is an open access article distributed under the terms and conditions of the Creative Commons Attribution (CC BY) license (<https://creativecommons.org/licenses/by/4.0/>).

1. Circular Dichroism (CD) and Proteins

1.1. CD

Many macromolecules exhibit molecular asymmetry, a phenomenon known as chirality. This characteristic entails that their three-dimensional structures cannot be superimposed onto their mirror images. In the context of molecular studies, chirality plays a crucial role in understanding the structural conformation and functional properties of bioactive molecules, including proteins, nucleic acids, and other complex biomolecules.

Circular dichroism (CD) spectroscopy is a powerful technique employed to explore and exploit this inherent chiral nature of molecules. In CD spectroscopy, a specialized light source emits circularly polarized light, which means that the electromagnetic vector oscillates in a rotational manner either to the right or to the left, forming a helical pattern around the axis of light propagation. This unique form of light can interact with chiral molecules in a distinct manner, leading to differential absorption of left-handed and right-handed circularly polarized light.

To elucidate chiral properties, CD spectroscopy typically employs circularly polarized light of both right-handed and left-handed orientations, which then passes through the sample of interest. By measuring the difference in absorption between these two components of light, researchers can derive valuable information about the chiral characteristics of optically active samples. Depending on the conformational asymmetry of the molecule, it

will exhibit varying degrees of differential absorption for left- and right-handed circularly polarized light. Seminal review articles on CD spectroscopy are available in the literature, such as those by Johnson [1], Kuwajima [2], and Koslowski et al. [3]. These articles provide excellent insights into the theoretical foundations, experimental techniques, and diverse applications of CD spectroscopy in the study of biomolecules. They explore the structure–function relationships and dynamics of biomolecules in various biological contexts.

1.2. Protein Conformation

CD spectroscopy is primarily applied for studying the secondary structure of proteins, although its applications extend to the investigation of peptide and nucleic acid conformations as well [1,4–6]. By measuring the differential absorption of left- and right-handed circularly polarized light, CD spectroscopy can distinguish between different types of secondary structure elements (Figure 1), such as alpha-helices, beta-sheets, and random coils, contributing to the overall conformation of the protein of interest. Noteworthy, a well-established resource for protein CD data is the Protein Circular Dichroism Data Bank (PCDDDB) [7,8], where validated spectra (Figure 1b), as well as related sources of information, are accessible.

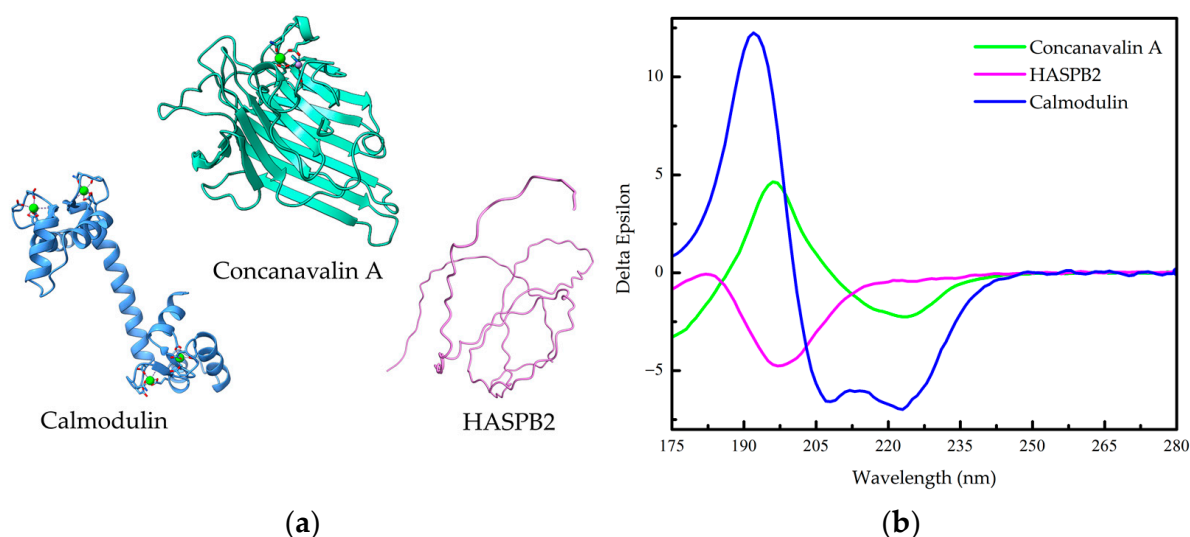


Figure 1. Secondary structure of proteins. (a) Helices: Calmodulin is formed mainly by α -helices (PDB 3CLN). Sheets: Concanavalin A is formed mainly by β -sheets (PDB 1JBC). Coils: Hydrophilic acylated surface protein B (HASPB2) is formed mainly by random coils (AlphaFold-generated structure from UniProt Q4QB56). (b) Far-UV circular dichroism (Far-UV CD) spectra of Calmodulin, Concanavalin A and HASPB2 from the The Protein Circular Dichroism Data Bank (PCDDDB) [7–10].

Figure 1b presents characteristic far-UV CD spectra for three types of protein secondary structures: an all- α -helix (Calmodulin), an all- β -sheet (Concanavalin A), and an all-random coil protein (HASPB2). In a CD spectrum, the absence of a signal indicates no circular dichroism, a negative signal signifies the absorption of left circularly polarized light, and a positive signal indicates the absorption of right circularly polarized light. The CD spectrum of an all- α -helical protein displays two prominent negative bands of approximately equal intensity at 222 and 208 nm, along with a positive band at around 190 nm (Figure 1b) [1,6]. The negative band at 222 nm arises due to the characteristic hydrogen-bonding environment of α -helices and remains relatively independent of their length [1,6]. On the other hand, the CD spectrum of an all- β -sheet protein typically exhibits a negative band spanning the wavelength range of 210–220 nm and a positive band between 195 and 200 nm (Figure 1b) [1]. The spectra for β -sheet proteins are more diverse compared to α -helical proteins, since β -sheets can adopt parallel, antiparallel, or mixed conformations and can exhibit various twisting arrangements [1]. It is worth mentioning

that the distinction between parallel and antiparallel β -sheets in a CD spectrum can be made by utilizing the BeStSel (β -structure selection) algorithm [11]. The CD spectrum of a random coil, or unfolded, protein displays a highly intense negative band at approximately 200 nm (Figure 1b), indicating disorderly conformation, a common feature in intrinsically disordered proteins (IDPs) such as HASPB2.

CD is used to study the secondary structure of proteins because the peptide bond is asymmetric, which means that it absorbs left-handed and right-handed circularly polarized light differently. The two electronic transitions of the amide chromophore that dominate the CD spectra of proteins are the $n \rightarrow \pi^*$ transition and the $\pi_0 \rightarrow \pi^*$ transition. The $n \rightarrow \pi^*$ transition is electrically prohibited but is magnetically permitted, which means that it is primarily responsible for the negative bands at 222 nm and 216–218 nm, which are characteristic of the α -helix and β -sheet spectra, respectively [6]. The $\pi_0 \rightarrow \pi^*$ transition is primarily responsible for the positive band at ~ 190 nm and the negative band at 208 nm, which are also characteristic of the α -helix spectrum, and for the positive band at ~ 198 nm, which is characteristic of the β -sheet spectrum [6].

For expressing CD spectroscopic results, the mean residue molar ellipticity, denoted as $[\theta]$, is used:

$$[\theta] = \frac{\theta \times 100 \times M}{C \times l \times N}, \quad (1)$$

where θ is the ellipticity in degrees, l is the optical path in cm, C is the concentration of protein in mg/mL, M is the molecular mass, and N is the number of residues in the protein [1]. The mean residue molar ellipticity ($[\theta]$) is given in $\text{deg cm}^2 \text{ dmol}^{-1}$. This standardization allows for independent comparison of results obtained from different sample batches or measured in various laboratories using different spectropolarimeters. This uniformity facilitates data exchange and collaboration among researchers, ensuring that CD spectroscopy remains a reliable and consistent technique in the scientific community. The expression of CD spectroscopy results can be employed to calculate $[\theta]$ values for various wavelengths, thereby generating a complete CD spectrum. In conventional CD instruments, a far-UV spectrum is collected from 180 to 250 nm. However, further information is available in the vacuum UV region (<180 nm), which can be collected using synchrotron radiation CD or SRCD [12].

To illustrate the aforementioned concepts, let us consider the properties of two proteins. The first one is sperm whale apomyoglobin, an all α -helical protein involved in oxygen transport, but in the apo form or without the heme (Figure 2a). Typically, a cell of 1 cm containing 2.4 micromolar (0.041 mg/mL) of the apoprotein, consisting of 153 residues with a molecular weight of approximately 17 kDa, exhibits a circular dichroism (CD) signal of -71 millidegrees (mdeg) at 222 nm [13,14]. This specific CD signal (Figure 2a) can be quantitatively related to the protein's secondary structure content using Equation (1):

$$[\theta]_{222} = \frac{-0.071 \times 100 \times 17000}{0.041 \times 1 \times 153} = -19240 \text{ deg cm}^2 \text{ dmol}^{-1}$$

The second protein is human DNAJA1, a heat shock co-chaperone involved with proteostasis (Figure 2b). A His-tagged DNAJA1, found as a roughly 94 kDa homodimer in solution with 417 amino acids per monomer, is a mixed α/β protein that exhibits a CD signal of about -17.5 mdeg at 222 nm from a 2 mm cell containing 6 micromolar (0.282 mg/L) of the purified protein, which in terms of mean residue molar ellipticity, by employing Equation (1), gives around $-3500 \text{ deg cm}^2 \text{ dmol}^{-1}$ [15].

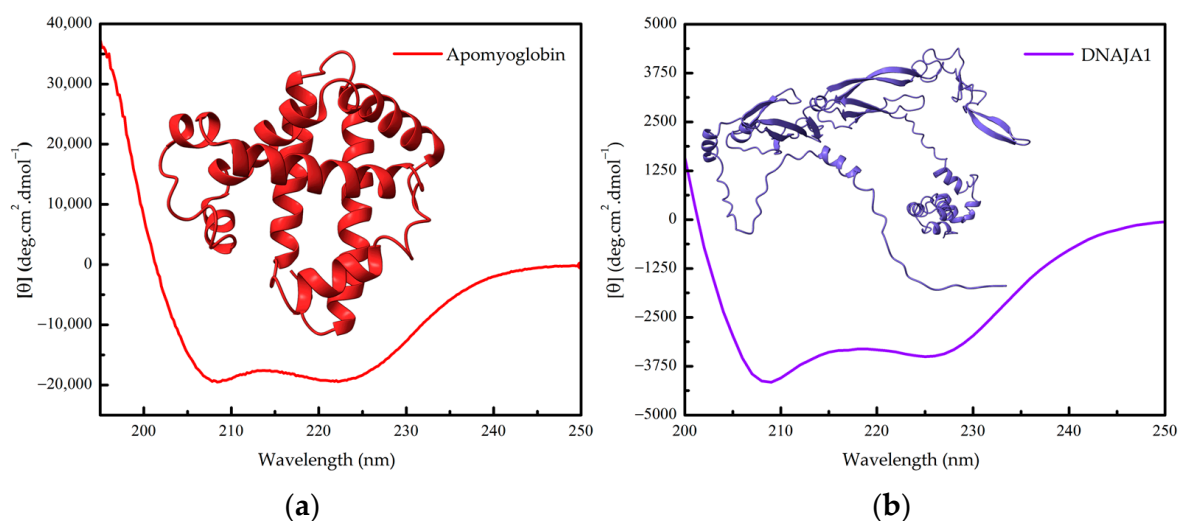


Figure 2. (a) Far-UV CD spectrum of apomyoglobin (without heme) and the three-dimensional structure of sperm whale myoglobin (PDB 5MBN). (b) Far-UV CD spectrum of human DNAJA1 and its three-dimensional structure (AlphaFold-generated structure from UniProt P31689).

In addition to its primary role in assessing protein secondary structure, circular dichroism can also offer valuable insights into aspects of protein tertiary structure, although its use for this purpose is less common. Aromatic residues, namely tryptophan, tyrosine, and phenylalanine, exhibit CD signals associated with $\pi_0 \rightarrow \pi^*$ electronic transitions in the range of 250 to 300 nm (see Figure 3). While these aromatic residues predominantly contribute to the near-UV CD spectra (wavelengths greater than 250 nm), they also have an impact on the far-UV spectra of proteins. In general, the contribution of aromatic residues to the far-UV CD spectra is relatively minor. However, when the protein contains a high concentration of these aromatic residues, the interpretation of the CD spectra becomes more complex, especially concerning the estimation of secondary structure elements (as discussed previously).

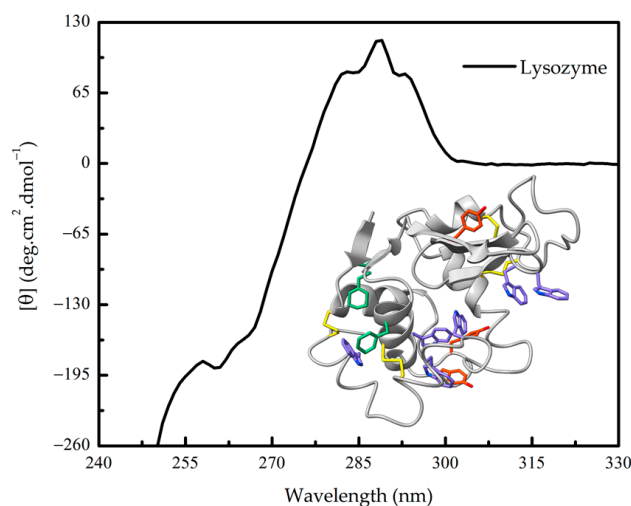


Figure 3. Near-UV circular dichroism (CD) spectra of hen egg-white lysozyme. The three-dimensional structure of lysozyme (PDB 1LYZ) and its near-UV chromophores phenylalanine (green), tyrosine (orange), tryptophan (violet) residues and cystine, is shown.

Another CD feature relevant to tertiary structure involves disulfide bonds. Disulfide bonds exhibit circular dichroism related to a transition from $n \rightarrow \sigma^*$ at approximately 260 nm. The CD peak associated with a disulfide bond is typically broader than that originating from

an aromatic residue. These tertiary structure-related CD signals provide complementary information to the primary focus on protein secondary structure analysis. However, due to the complexity introduced by high aromatic residue content and the presence of disulfide bonds, careful interpretation and analysis are required when studying tertiary structural aspects using circular dichroism.

Near-ultraviolet (near-UV) CD absorption in proteins is primarily mediated by chromophores, which constitute a minor fraction of the amino acid composition. Therefore, achieving reliable results in this spectral range requires a combination of increased chromophore concentration and/or an extended optical path length. Because tryptophan residues are the primary contributors to chromophoric properties in this spectral region, the adjustment of this combination should be based on their abundance to ensure optimal spectroscopic conditions (see Section 2: Fine-Tuning Experimental Parameters for Accurate Results). Researchers must meticulously account for these factors in their experimental design to obtain precise and meaningful insights into the overall structure and functionality of proteins.

It is also worth noting that Circular Dichroism (CD) can be effectively combined with various other biophysical techniques to explore protein dynamics and the intricate relationship between conformation and function. While we can only briefly mention a few of these complementary methods, they play a crucial role in expanding our understanding. For instance: tryptophan fluorescence spectroscopy, which allows for the assessment of residue environments; extrinsic fluorescence, utilized to measure the exposure of hydrophobic surfaces, among other applications; Size Exclusion Chromatography coupled with Multi-Angle Light Scattering (SEC-MALS), providing precise information on molecular mass; Analytical Ultracentrifugation, capable of measuring sedimentation (*s*) and diffusion (*D*) coefficients, while also offering insights into oligomerization in equilibrium; and Small-Angle X-ray Scattering (SAXS), providing low- to medium-resolution information on shape, among many others. Interested readers are encouraged to explore dedicated reviews on these techniques [16–21] for in-depth insights into their applications in the study of proteins.

1.3. Further Advantages of CD Spectroscopy in Protein Research

Circular dichroism is widely applied in the study of proteins, particularly for estimating their secondary structure. With significant advancements in cloning and purification techniques, the production of numerous proteins has become feasible. However, obtaining high-resolution structural information through X-ray diffraction or nuclear magnetic resonance can sometimes be challenging or even unattainable due to technical limitations.

While CD cannot match the level of detail provided by these advanced techniques, it excels in offering valuable estimations of the proportion of residues involved in α -helix, β -sheet, or disorderly formations within a protein's structure. This aspect is particularly valuable when high-resolution structural data is unavailable. Furthermore, even when such information exists (a subject that has gained strength over recent years with the advancement of artificial intelligence-based methods such as AlphaFold and RoseTTAFold providing highly accurate predicted models [22,23]), CD provides crucial additional insights into the impact of various factors, such as temperature [24,25], pH [14,16,26], charge [27], ligands [28–34], protein/peptide binding [35,36], mutations [33,37,38] and others on protein secondary structure. This is because CD is a sensitive technique that can detect subtle changes in protein conformation, even when these changes are not large enough to be observed in high-resolution structural data.

Another essential advantage of CD spectroscopy is its nondestructive nature, making it particularly valuable for investigating protein folding and the intricate processes of protein–protein and protein–DNA interactions [1,39]. The nondestructive nature of CD allows researchers to monitor these interactions in real-time and under various experimental conditions, providing valuable insights into the structural stability and functional behavior of proteins. Another significant advantage of CD spectroscopy is its ability to achieve meaningful results with concentrations ranging from 1 to 10 mg/mL. This characteristic

is particularly valuable when working with limited or precious samples, as it minimizes sample consumption while still providing robust structural information.

Moreover, CD spectroscopy has found a widespread application in elucidating the binding mechanisms and conformational changes that occur during protein–protein interactions and protein–DNA interactions. By analyzing the differential absorption of circularly polarized light, researchers can derive valuable information about the secondary structure alterations and conformational rearrangements that take place upon binding to other biomolecules.

1.4. Predicting Protein Secondary Structure: Computational Analysis of CD Spectra

It is important to note that these CD spectral patterns are fundamental in assessing protein secondary structure and can be utilized to gain valuable insights into the conformational characteristics of proteins. For up-to-date applications, advancements in CD spectroscopy, coupled with computational approaches and refined algorithms, continue to enhance our understanding of protein structures and their functional implications. Computational methods can also be used to analyze CD spectra and to estimate the secondary structure content of proteins.

Numerous methods have been developed to predict a protein's secondary structure from its CD spectrum, relying on statistical and/or physical–chemical information derived from the protein's primary sequence. In particular, the fractional helicity (fH) or the mole fraction of helical backbone α -carbons within the peptide or protein is commonly calculated in proportion to the experimental molar residue ellipticity at 222 nm ($[\theta]_{222}$) [40]. Among these methods, a straightforward yet reasonably reliable approach for estimating the α -helix content involves evaluating the signal at 222 nm using Equations (2) [41] or (3) [42] shown below:

$$fH = \frac{[\theta]_{222} - 3000}{(-36000 - 3000)}, \quad (2)$$

$$[\theta]_{222} = \left(fH + \frac{iK}{N} \right) \times [\theta]_{HX}, \quad (3)$$

where $[\theta]_{222}$ is the mean molar residual ellipticity at 222 nm (in $\text{deg cm}^2 \text{dmol}^{-1}$), fH is the fractional helicity (in %), i is the number of helices in the protein, K is a constant at 222 nm that is equal to 2.57, N is the number of residues in the proteins, and $[\theta]_{HX}$ is the mean residue molar ellipticity when 100% of the structure is α -helical. The experimental molar residue ellipticity at 222 nm ($[\theta]_{HX}$) is quantified as $-34,686 \text{ deg cm}^2 \text{dmol}^{-1}$, which represents the theoretical maximum value for an all- α -helical protein. This valuable reference point allows for meaningful comparisons with obtained experimental results. For instance, if the calculated value significantly exceeds this theoretical maximum or is equal to it, and there are previous indications suggesting that the protein's conformation should not be 100% helical, it necessitates a thorough revision of the experimental setups and calculations. Moreover, CD signals between 215 and 220 nm can be used to predict the maximum value for a 100% β -sheet protein, which is approximately $-20,000 \text{ deg cm}^2 \text{dmol}^{-1}$. This information proves useful in assessing and interpreting CD results related to β -sheet-rich protein conformations.

Additionally, Greenfield and Fasman [43] demonstrated that both β -sheets and random coils exhibit low ellipticity at 208 nm, approximately $-4000 \text{ deg cm}^2 \text{dmol}^{-1}$, whereas an α -helix displays a maximum ellipticity at 208 nm, around $-33,000 \text{ deg cm}^2 \text{dmol}^{-1}$. Consequently, they proposed that an approximate estimation of the α -helical content may be derived from $[\theta]_{208}$, the mean molar residue ellipticity in $\text{deg cm}^2 \text{dmol}^{-1}$ at 208 nm:

$$fH = \frac{[\theta]_{208} - 4000}{(-33000 - 4000)}, \quad (4)$$

Various methods exist that utilize the entire spectrum of a protein to predict its secondary structure content. It is essential to underscore that errors in calculating the

protein concentration can result in corresponding errors or even larger discrepancies in predicting the protein's secondary structure. Therefore, accurate determination of protein concentration is crucial for reliable predictions.

There are several tools and methods available for predicting secondary structure from circular dichroism (CD) spectra. Two notable examples of web platforms designed for protein analysis are the Beta Structure Selection (BeStSel) [11] server and DichroWeb [44]. Both platforms can handle the spectral diversity of proteins and are widely used in analytical processes. BeStSel's method is specifically tailored for the analysis of β -rich and soluble proteins, and DichroWeb offers a wide range of reference datasets and algorithms for secondary structure calculation. These websites allow users to directly input experimental spectra data from both conventional circular dichroism (CD) and synchrotron radiation circular dichroism (SRCD). This data, along with the associated parameters, enables the generation of secondary structure percentages. Additionally, these platforms include an assessment mechanism to evaluate the quality of fit between predicted and experimental data.

Another significant tool for predicting protein secondary structure is K2D3 [45], a neural network-based method available through a public web server. K2D3 uses its own theoretical CD reference dataset to estimate α -helix and β -sheet content from protein CD data in the 190–240 nm range. Optionally, it can also perform estimates based on the size of the analyzed protein, either in the number of amino acids or in molecular weight (in kDa).

Finally, it is also possible to predict CD spectra from protein atomic coordinates (see, for instance [46,47]). For example, the computational method SESCO (Structure-Based Empirical Spectrum Calculation Algorithm) was successfully used to add CD information to AlphaFold predicted models recently (see reference [48]). These packages play a crucial role by providing users with predicted CD spectra of proteins in cases where the acquisition of experimental CD spectra is unattainable.

2. Fine-Tuning Experimental Parameters for Accurate Results

The circular dichroism (CD) spectrum of a protein is contingent upon both its conformational arrangement and concentration. An accurate determination of concentration holds a pivotal significance in the prognosis of secondary structural attributes. Discrepancies in concentration measurements by approximately 10% introduce commensurate errors in structural prognostications that can lead to misclassifications. Among the prevailing methodologies for quantifying protein concentrations, the method proposed by Edelhoch remains a dependable choice [16,49,50].

The Edelhoch method [51] is straightforward and practical, rendering it suitable for implementation in any experiment. It is based on the absorbance spectra of the aromatic groups of protein, namely tyrosine (Y) and tryptophan (W), and disulfides from cystine (CySS). The molar absorbance coefficients (ϵ) at 280 nm are computed in a 20 mM phosphate buffer at pH 6.5, along with 6 M Gdm-Cl. The count of these residues (nAA, number of amino acid) in a protein is then determined, and the ϵ of the protein is calculated using Equation (5):

$$\epsilon_{280}(\text{protein}) = [5690 \times (nW)] + [1280 \times (nY)] + [125 \times (nCySS)], \quad (5)$$

The assessment of protein concentration is also pivotal in optimizing the signal-to-noise ratio. As a preliminary approximation, for a pathlength of 0.1 mm, a concentration of 0.1% (w/v) is suggested, while for a pathlength of 1 mm, a concentration of 0.01% (w/v) is deemed suitable [52]. Although these values can vary depending on the folding state of the protein, they serve as a good starting point for initial measurements. Furthermore, an essential preliminary step is to measure the absorption of the sample at the wavelength of interest for CD experimentation. An optimal absorbance value of 0.87 is recommended, as it yields the highest signal-to-noise ratio. It is advisable to avoid absorbance readings surpassing 1.2. For a comprehensive catalog of absorbance values for a protein solution (1 mg/mL) within a 1 cm pathlength cell across various ultraviolet wavelengths, please refer to [53].

In an ideal scenario, proteins should undergo dilution in either pure water or, at the very least, a 10 mM phosphate solution. However, numerous proteins demonstrate insolubility under these conditions, necessitating the inclusion of supplementary agents. Irrespective of this, it is imperative that the buffers employed for protein dilution maintain exceptional transparency. This is particularly crucial since the evaluation of secondary structure entails measurements at wavelengths below 240 nm, wherein various buffers exhibit light-absorbing characteristics. Consequently, the chemical constituents engaged in buffer formulation must exhibit a high degree of purity, devoid of impurities capable of light scattering. When required, the buffers should be meticulously filtered to eliminate particulate matter. Solutions containing NaClO_4 , NaF, or KF at a concentration of 10 mM exhibit a nearly complete absence of light absorption at wavelengths extending down to 170 nm, especially when examined using a 1 mm cell as outlined by Schmid [52]. Common reducing agents such as DTT (Dithiothreitol) and BME (Beta-mercaptoethanol), which are used to disrupt disulfide bonds, must be present in a low concentration in buffers used for far-UV CD analysis. But, because they absorb light in this region, a suitable alternative is TCEP (Tris(2-carboxyethyl)phosphine), which has low absorptivity in this region. Additional comprehensive insights are available in other references [30,53–55].

Various additives are frequently employed to augment the propensity of specific polypeptides towards adopting secondary structures. These include trifluoroethanol (TFE), hexafluoroisopropanol, ethylene glycol, glycerol, and others. Notably, TFE stands out as the most extensively utilized compound in this regard [56]. Elevated TFE concentrations resulted in a notable increase in the $[\theta]_{222}$ parameter of apomyoglobin [55]. While TFE is commonly employed at elevated concentrations (up to 100%) for peptide analysis [57], the same approach is discouraged for proteins. Prior observations have demonstrated that concentrations exceeding 10% have a deleterious impact on protein tertiary structure, thereby compromising its native state. The stability of proteins is notably altered by small, viscosity-inducing co-solvents [58]. A study encompassing a range of small, viscosity-inducing co-solvents on apomyoglobin revealed that increasing the sucrose concentration led to a heightened CD signal across the entire spectrum, thus impacting the secondary structure specifically [34]. This effect was distinct from tertiary structure alterations, as ascertained through the investigation of ^1H one-dimensional nuclear magnetic resonance (NMR) spectra [34]. Secondly, the study probed stability by tracking urea-induced unfolding using $[\theta]_{208}$ to assess conformation. The results indicated that viscogenic co-solvents enhance the stability of apoMb pH 4 intermediate in comparison to the urea-induced unfolded form [34]. Consequently, viscogenic co-solvents offer a viable avenue to stabilize protein preparations that exhibit partial unfolding, signifying their potential utility in such scenarios.

The quantification of light absorption is manifested through the dynode voltage module (in volts, V), a metric that quantifies the photomultiplier's response during measurement. This value correlates with the quantity of photons either unabsorbed or scattered by the specimen. A higher recorded value signifies augmented absorption or scattering. Elevated absorption triggers amplified noise, consequently heightening the imprecision in elasticity measurements. Typically, a dependable threshold for readings rests at 600 V, yet acquisitions extending up to 700 V can be admissible, provided a sufficiently extensive collection and accumulation of spectra are undertaken to mitigate the noise originating from absorption effects. It is prudent to refrain from conducting readings with voltages surpassing 700 V, as this could potentially impair the instrumentation.

The cuvettes utilized should be constructed from quartz material to accommodate ultraviolet wavelength measurements. Handling the cuvettes with gloves is recommended to minimize contamination. Premium-grade cuvettes exhibit near-total transparency. Verification of the cuvette's integrity can be carried out by comparing readings obtained from an empty cuvette with those from the empty sample holder, both of which should yield analogous measurements reflecting the presence of air alone. Cleaning cuvettes can be achieved using ethanol or organic solvents like acetone, albeit with meticulous attention

to eliminate any residual substances. Additionally, specialized commercial detergents designed for cuvette cleaning are available. Immersion in 50% nitric acid for an extended duration may be essential to dislodge protein adherents from the quartz surfaces [59].

A consistent nitrogen flow should be maintained during measurements, typically set at 3 L/min for 260 nm, 5 L/min for the 200–260 nm range, 10 L/min for 180–200 nm, and 50 L/min for 180 nm. The lamp should be allowed to operate for a minimum of 30 min, with the optimal duration being 60 min, prior to initiating measurements. Calibration of the instrument employs the standard D(+)-camphorsulfonic acid, wherein a concentration of 0.6 mg/mL yields an absorption of 188 mdeg at 290.5 nm within a 1 cm cell, and -38 mdeg at 192.5 nm within a 1 mm cell. D(–)-pantolactone is a similarly effective standard in the UV range, with a 0.03% aqueous solution generating a signal of -186 mdeg at 219 nm using a 1 cm pathlength cell.

Optimal instrumental settings are critical for minimizing the signal-to-noise ratio. The spectral bandwidth, governed by the slit width, should be maximized without inducing distortion in the spectral bands. Conducting a series of preliminary scans with progressively larger slit settings aids in determining the maximum slit width prior to encountering absorbance reduction. Additionally, signal-to-noise enhancement is proportional to the square root of the integration time. Consequently, enhancing spectrum quality can be achieved by increasing the response time. However, this requires a corresponding reduction in reading speed to ensure that the product of reading speed and response time remains below the chosen bandwidth for the experiment. For example, at a reading speed of 200 nm/min, the response time should be 0.1 s; for a reading speed of 50 nm/min, it should be 1 s (considering bandwidth values of 0.5 nm and 1 nm, respectively). Noise reduction can also be attained through an accumulation of readings. In this context, to augment the signal-to-noise ratio by a factor of X , the accumulation time should be X^2 . Alterations to solvent type, sample concentration, and optical pathlength are alternative avenues to refine the quality of the obtained spectrum.

For initial protein analysis, suggested measurement parameters include a spectral bandwidth of 2 nm for the far-UV region and 1 nm for the near-UV region, a response time of 1 s, and a scanning speed of 20 nm/min. The accumulation count of spectra should be adjusted based on necessity, and each spectrum measurement should extend to where HT (high tension) reaches approximately 700 V. Running the sample prior to the buffer baseline optimizes the subsequent subtraction by maintaining uniform parameters.

3. Studying Protein Unfolding and Aggregation Dynamics under Denaturing Conditions

CD spectroscopy is widely employed to monitor protein stability under escalating denaturing conditions. Common denaturants encompass temperature, chemical agents (typically urea and guanidinium chloride), and extreme pH conditions (usually acidic). As the denaturant intensity rises, protein stability decreases, ultimately culminating in unfolding [60]. CD proves a practical method for tracking protein unfolding, as the spectra of folded proteins and random coils exhibit pronounced disparities, and the unfolding transition can be readily discerned by selecting a wavelength where the signal divergence between folded and unfolded protein states is substantial. For example, α -helical proteins display a pronounced CD signal at 222 nm, whereas unfolded proteins manifest little-to-no signal at the same wavelength. In one example, the CD signal was employed at a wavelength of 222 nm to track the unfolding process of the RNase A protein [6]. This monitoring was conducted under varying conditions, including alterations in temperature and the introduction of escalating concentrations of urea. Figure 3 within this publication illustrates the transition profiles of RNase A unfolding in two distinct scenarios: one in the absence of any additives and the other in the presence of 200 mM Na_2SO_4 . The depicted data demonstrates that the introduction of the salt leads to an augmentation in the stability of RNase A when it undergoes unfolding induced by either changes in temperature or the application of high urea concentrations.

In another example, far-UV CD at a wavelength of 222 nm was harnessed to meticulously track both the folding and unfolding processes of the N-terminal domain of the TnC protein [61]. This measurement was significant as it illuminated the reversible nature of the unfolding of the domain, as evidenced by the convergence of the obtained curves. In this case, unfolding was also investigated using near-ultraviolet circular dichroism (near-UV CD) at a wavelength of 270 nm, which specifically monitors tertiary interactions within the protein structure. The results indicated that, during the unfolding process, the tertiary structure underwent destabilization prior to alterations in the secondary structure. Notably, the observed curves did not align precisely, serving as a critical revelation that the unfolding behavior of the protein did not conform to a two-state unfolding profile.

CD also serves as a valuable tool for monitoring aggregation during heat-induced unfolding. The dynode voltage (V)—a high voltage applied to the photomultiplier of the UV detector to counterbalance diminishing light intensity—reflects light absorption or scattering and is requisite for all CD measurements. When correlated with scattering, the recorded dynode voltage (V) can serve as a measure of solution turbidity [62]. In a planned experimental setup, both the CD signal at 222 nm and the dynode voltage (V) are concurrently recorded as functions of temperature. The recorded curve profile in this context reveals a decrease in the CD signal, which is indicative of the unfolding of the protein and the subsequent loss of its secondary structure. Furthermore, the subsequent increase in dynode voltage, signifying an elevation in light scattering, implies the concurrent occurrence of protein aggregation. This dual observation suggests that, in addition to the unfolding process and the concomitant loss of secondary structure, there is also a propensity for protein aggregation to take place in the sample.

4. Synchrotron Radiation Circular Dichroism (SRCD) Spectroscopy

In recent years, the use of synchrotron radiation as a light source for CD measurements has gained traction, offering enhanced sensitivity and resolution. There are several excellent reviews that explain the technique and its applications in detail (see [63–65], to name a few).

As mentioned in the previous section of this review, many factors affect CD measurement, resulting in a decrease in the signal-to-noise (S/N) ratio, especially at lower wavelengths. Scattering light from buffer composition, high protein concentration, etc., are true factors that decrease S/N and limit the minimum wavelength in which it is possible to get reliable data on the CD spectrum of a protein. Even the air can contribute to poor data from readings. Measurements at lower wavelengths are essential to generate more refined data on the secondary structure.

Synchrotron light sources are advanced particle accelerators designed to produce extremely intense and highly focused beams of light across a wide range of wavelengths, from infrared to X-rays. One of the major advantages of synchrotron light is its ability to span a broad range of wavelengths, from the visible to hard X-rays, each with very high brilliance. This extreme brightness allows researchers to study samples at very high resolutions, and its ability to span a broad range of wavelengths allows researchers to use it for a wide variety of applications (see, for instance, Figure 4).

The superiority of SRCD over conventional CD results in a large increment in the data produced and consequently in our understanding of the secondary structure of proteins. SRCD offers the capability to collect data at lower wavelengths (<190 nm), which encompass more electronic transitions and thus provide a richer source of structural information. This is particularly beneficial for determining secondary structure profiles, since a more detailed spectrum allows algorithms to more accurately discern the types of secondary structures composing a protein. Also, owing to the higher photon flux in SRCD, it exhibits a superior signal-to-noise ratio. This means that SRCD can deliver reliable results with smaller sample quantities and is better equipped to handle issues related to buffer transparency and necessary additives. Furthermore, SRCD in principle performs exceptionally well in the presence of absorbent buffers, lipids, and detergents. Consequently, SRCD excels

in characterizing even subtle conformational changes. These advantages make SRCD particularly valuable for assessing protein stability and detecting ligand binding.

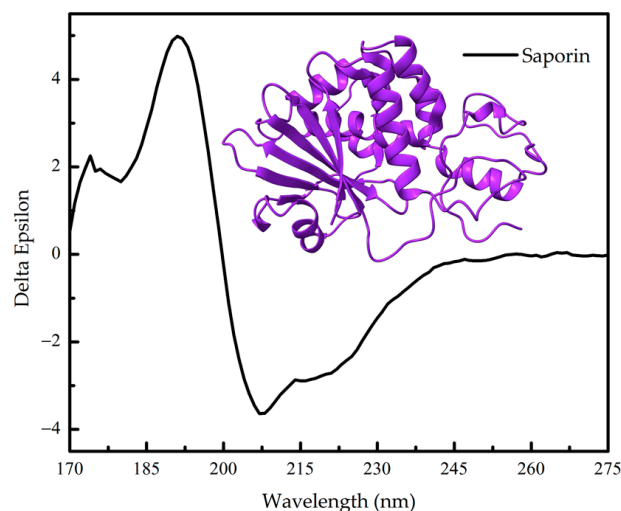


Figure 4. Far-UV circular dichroism (CD) spectrum of ribosome-inactivating protein Saporin-6 (UniProt P20656) from the The Protein Circular Dichroism Data Bank (PCDDDB) [8,9] and its three-dimensional structure (PDB 1QI7).

A few recent examples of this use follow. SRCD, combined with a stopped-flow apparatus, was used to follow the formation of a helical structure in the coupled folding and binding reaction between two protein domains, the interaction domain from the activator of thyroid hormone and retinoid receptors (ACTR) and the nuclear coactivator binding domain (NCBD) from the CREB-binding protein (CREBBP) [66]. The study showed that folding and binding reactions are coupled in this system, i.e., an initial association that leads to helix formation is coupled with slower kinetic phases, which likely arise from subtle rearrangements of helical complexes. SRCD experiments in equilibrium were down to 180 nm, and kinetics were followed at 195 nm.

SRCD was used to investigate both the folded state and the stability of the Hsp70-Hsp90 organizing protein (Hop) from *P. falciparum* Hop, showing that it is unstable at temperatures higher than 40 °C [67]. SRCD spectra of the apo and holo forms of a Rubredoxin protein class of iron-sulfur proteins from *Marinobacter hydrocarbonoclasticus* are different (down to 180 nm) and are interconverted upon metal incubation [68]. SRCD was also used to study the folding and unfolding kinetics of pepsin under oxidative conditions to understand how this condition impacts the pepsin secondary structure and its hydrolytic activity [69].

In addition, SRCD was used to demonstrate that Au and Ag nanoparticles can cause conformational changes in the structure of a key component of surfactant protein B, which plays a key role in the biophysical function of lung surfactant and is essential to life, which could change its effect *in vivo*, potentially leading to alterations in lung surfactant function and ultimately the physiological behavior of the lung [70]. In this case, most of the spectral change occurs below 210 nm. As for CD, SRCD is also used to study nucleic acid conformation [71]. Pertinent spectroscopic data can be accessed through the Nucleic Acid Circular Dichroism Database (NACDDB). This public repository encompasses both CD and SRCD data for a variety of nucleic acid molecules [72].

5. Solid-State (SSCD), Vibrational (VCD) and High-Throughput (HTC) Circular Dichroism Spectroscopy

There is a justifiable interest in the application of circular dichroism in solid-state analysis, particularly due to its relevance in studying bioactive compounds with potential applications in biotechnology and medicine [73,74]. In the solid state, molecular interactions display significantly enhanced strength compared to the solution phase, thereby positively

influencing chirality. This phenomenon makes solid-state circular dichroism (SSCD) an optimal method for the study of materials. As a result, SSCD, a specialized form of CD spectroscopy, has emerged as a powerful and straightforward technique for investigating various aspects of optically active organic and inorganic molecules [75]. It is important to note, however, that, while SSCD is a powerful tool, it is not without limitations, and artifact signals can be quite pronounced. Careful attention must be paid when employing conventional CD equipment for measurements on solid-state samples [74]. To address these challenges, specialized accessories such as solid-state sample holders and lens units, as well as specific analysis techniques based on the Stokes–Mueller matrix analysis, have been developed to facilitate measurements and their interpretation [73,76].

SSCD has found numerous applications in the study of proteins. For instance, it has been employed to investigate the integration of globular proteins into 3D-printed bioplastics with unique mechanical properties. CD spectroscopy was used to examine the conformation of Bovine Serum Albumin (BSA) in both aqueous resin and bioplastic, revealing the preservation of the folded conformation [75]. Given that even globular proteins can transition into amyloidogenic states, typically forming insoluble fibrils [77], it becomes imperative to understand the relationship between these two states. This understanding is vital for designing strategies to modulate the process for biotechnological and medicinal purposes, and SSCD has proven invaluable in these investigations [78]. SSCD results have demonstrated that certain proteins undergo structural rearrangements from the solution phase to the solid state, adopting a beta-sheet structure and becoming more compact [78]. This approach has also been applied to the study of peptides, revealing that, at least in shorter chains, the type of secondary structure formed under amyloidogenic conditions may be sequence-dependent [78,79]. CD has also been used to access protein/peptide folding in semisolid biomaterials, such as hydrogels [80–82].

A more comprehensive investigation of protein secondary structure can be achieved through the use of vibrational circular dichroism (VCD) spectroscopy. This tool expands the traditional wavelength range, enabling the measurement of infrared fingerprints. In essence, it extends into the infrared and near-infrared regions [83–86]. As for its relatively weak signal, recent approaches have been successful in addressing this limitation [87,88]. Moreover, numerous studies have reported on the conformational properties of various proteins in solution [88–90]. VCD spectra are highly sensitive to molecular structure, providing valuable insights into conformation. They can be effectively utilized to assess the impact of various perturbations on conformation, such as mutations, changes in buffer composition, temperature variations, ligand binding, and more [91–93].

Recent advancements have given rise to a system known as high-throughput circular dichroism (HTCD), which can accommodate 96-well plates maintained at controlled temperatures before measurement. The most significant development lies in the automation of this process, enabling the evaluation of a large number of protein and biomolecule samples. Software plays a crucial role in the measurement process, as it generates data acquisition sequences and scan parameters, including wavelength and temperature scans. Furthermore, the software is instrumental in the analysis phase, offering information on quality control and secondary structure estimation. For more details and application notes, please visit the following website: https://jascoinc.com/applications/?_sf_s=HTCD&_sft_technique-category=circular-dichroism-applications (accessed on 21 November 2023). The application notes cover a range of topics, including results with automated CD and fluorescence, quality control and conformational measurements, thermal-induced unfolding, ligand binding, and the effect of buffer conditions.

This is only a concise overview of the subject of SSCD, VCD, and HTCD, and is not intended to comprehensively cover the entire field on these techniques and their intricate details. The objective is to introduce the reader to these valuable methods and provide references to a select few reviews and works, considering the constraints of space.

6. Conclusions

In modern research, CD spectroscopy continues to be an indispensable tool for studying the conformational changes in proteins and their dynamic interactions with other biomolecules. Advantages of CD spectroscopy are that it is non-destructive, rapid, and sensitive to changes in secondary structure. Overall, CD spectroscopy remains a powerful and versatile technique in the study of biomolecular interactions, contributing to the advancement in our understanding of essential biological processes and facilitating the development of targeted therapeutics and biomedical applications.

As research advances and instrumentation improves, CD spectroscopy continues to be an indispensable tool for structural biologists, providing fundamental information about the conformation and dynamics of biomolecules. Moreover, its nondestructive nature makes it an attractive option for studying sensitive or complex macromolecular systems. Researchers can confidently utilize CD spectroscopy to elucidate the structural properties of proteins, peptides, nucleic acids, and other biomolecules, paving the way for deeper insights into their functions and interactions within complex biological processes. Furthermore, CD spectroscopy enables researchers to examine a wide range of experimental conditions, such as temperature, pH, the presence of various ligands, and solid and semi-solid samples. This flexibility in studying multiple variables empowers scientists to gain a comprehensive understanding of how the protein's conformation responds to different environmental conditions and ligand binding.

In summary, CD has proven to be an invaluable tool for gaining insights into protein secondary structure, especially when higher-resolution structural information is limited. Its ability to shed light on how various factors influence protein conformation makes it a valuable asset, even in cases where detailed structural data are available through other methods. With its numerous advantages, CD spectroscopy has become an essential tool in the field of structural biology.

Author Contributions: Conceptualization, L.A.L. and C.H.I.R.; writing—original draft preparation, L.A.L. and C.H.I.R.; writing—review and editing, L.A.L. and C.H.I.R.; supervision, C.H.I.R.; project administration, C.H.I.R.; funding acquisition, C.H.I.R. All authors have read and agreed to the published version of the manuscript.

Funding: This study was supported by FAPESP, grant numbers 2012/50161-8 and 2017/26131-5; and CNPq, grant number 305148/2019-2, awarded to C.H.I.R. L.A.L. thanks CAPES for their fellowship, grant number 88887.682850/2022-0.

Conflicts of Interest: The authors declare no conflict of interest.

References

1. Johnson, W.C. Circular dichroism and its empirical application to biopolymers. *Methods Biochem. Anal.* **1985**, *31*, 61–163. [[CrossRef](#)]
2. Kuwajima, K. Circular Dichroism. *Methods Mol. Biol.* **1995**, *40*, 115–135. [[CrossRef](#)] [[PubMed](#)]
3. Koslowski, A.; Sreerama, N.; Woody, R.W. Theoretical Approach to Electronic Optical Activity. In *Circular Dichroism: Principles and Applications*, 2nd ed.; Berova, N., Ed.; John Wiley & Sons, Inc.: New York, NY, USA, 2000; pp. 55–96.
4. Woody, R.W. Circular dichroism. *Methods Enzymol.* **1995**, *246*, 34–71. [[CrossRef](#)] [[PubMed](#)]
5. Woody, R.W. Theory of circular dichroism of proteins. In *Circular Dichroism and the Conformational Analysis of Biomolecules*; Fasman, G.D., Ed.; Plenum Press: New York, NY, USA, 1996; pp. 25–67.
6. Woody, R.W.; Koslowski, A. Recent developments in the electronic spectroscopy of amides and α -helical polypeptides. *Biophys. Chem.* **2002**, *101–102*, 535–551. [[CrossRef](#)]
7. Whitmore, L.; Woollett, B.; Miles, A.J.; Klose, D.P.; Janes, R.W.; Wallace, B.A. PCDDb: The protein circular dichroism data bank, a repository for circular dichroism spectral and metadata. *Nucleic Acids Res.* **2010**, *39*, D480–D486. [[CrossRef](#)] [[PubMed](#)]
8. Ramalli, S.G.; Miles, A.J.; Janes, R.W.; Wallace, B. The PCDDb (Protein Circular Dichroism Data Bank): A Bioinformatics Resource for Protein Characterisations and Methods Development. *J. Mol. Biol.* **2022**, *434*, 167441. [[CrossRef](#)] [[PubMed](#)]
9. Lees, J.G.; Miles, A.J.; Wien, F.; Wallace, B.A. A reference database for circular dichroism spectroscopy covering fold and secondary structure space. *Bioinformatics* **2006**, *22*, 1955–1962. [[CrossRef](#)]
10. Miles, A.J.; Drew, E.D.; Wallace, B.A. DichroIDP: A method for analyses of intrinsically disordered proteins using circular dichroism spectroscopy. *Commun. Biol.* **2023**, *6*, 823. [[CrossRef](#)] [[PubMed](#)]

11. Micsonai, A.; Wien, F.; Kernya, L.; Lee, Y.-H.; Goto, Y.; Réfrégiers, M.; Kardos, J. Accurate secondary structure prediction and fold recognition for circular dichroism spectroscopy. *Proc. Natl. Acad. Sci. USA* **2015**, *112*, E3095–E3103. [[CrossRef](#)]
12. Wallace, B.; Janes, R.W. Synchrotron radiation circular dichroism spectroscopy of proteins: Secondary structure, fold recognition and structural genomics. *Curr. Opin. Chem. Biol.* **2001**, *5*, 567–571. [[CrossRef](#)]
13. Ramos, C.H.I.; Kay, M.S.; Baldwin, R.L. Putative Interhelix Ion Pairs Involved in the Stability of Myoglobin. *Biochemistry* **1999**, *38*, 9783–9790. [[CrossRef](#)] [[PubMed](#)]
14. A Ribeiro, E.; Ramos, C.H. Origin of the anomalous circular dichroism spectra of many apomyoglobin mutants. *Anal. Biochem.* **2004**, *329*, 300–306. [[CrossRef](#)] [[PubMed](#)]
15. de Jesus, J.R.; Linhares, L.A.; Aragão, A.Z.; Arruda, M.A.; Ramos, C.H. The stability and function of human cochaperone Hsp40/DNAJA1 are affected by zinc removal and partially restored by copper. *Biochimie* **2023**, *213*, 123–129. [[CrossRef](#)]
16. Ramos, C.H.I. A spectroscopic-based laboratory experiment for protein conformational studies. *Biochem. Mol. Biol. Educ.* **2004**, *32*, 31–34. [[CrossRef](#)]
17. Silva, J.L.; Oliveira, A.C.; Vieira, T.C.R.G.; de Oliveira, G.A.P.; Suarez, M.C.; Foguel, D. High-Pressure Chemical Biology and Biotechnology. *Chem. Rev.* **2014**, *114*, 7239–7267. [[CrossRef](#)] [[PubMed](#)]
18. Batista, F.A.; Gava, L.M.; Pinheiro, G.M.S.; Ramos, C.H.; Borges, J.C. From Conformation to Interaction: Techniques to Explore the Hsp70/ Hsp90 Network. *Curr. Protein Pept. Sci.* **2015**, *16*, 735–753. [[CrossRef](#)]
19. Borges, J.C.; Ramos, C.H. Analysis of molecular targets of Mycobacterium tuberculosis by analytical ultracentrifugation. *Curr. Med. Chem.* **2011**, *18*, 1276–1285. [[CrossRef](#)]
20. Guo, H.; An, S.; Ward, R.; Yang, Y.; Liu, Y.; Guo, X.-X.; Hao, Q.; Xu, T.-R. Methods used to study the oligomeric structure of G-protein-coupled receptors. *Biosci. Rep.* **2017**, *37*, BSR20160547. [[CrossRef](#)]
21. Borges, J.C.; Seraphim, T.V.; Dores-Silva, P.R.; Barbosa, L.R.S. A review of multi-domain and flexible molecular chaperones studies by small-angle X-ray scattering. *Biophys. Rev.* **2016**, *8*, 107–120. [[CrossRef](#)]
22. Jumper, J.; Evans, R.; Pritzel, A.; Green, T.; Figurnov, M.; Ronneberger, O.; Tunyasuvunakool, K.; Bates, R.; Židek, A.; Potapenko, A.; et al. Highly accurate protein structure prediction with AlphaFold. *Nature* **2021**, *596*, 583–589. [[CrossRef](#)]
23. Baek, M.; DiMaio, F.; Anishchenko, I.; Dauparas, J.; Ovchinnikov, S.; Lee, G.R.; Wang, J.; Cong, Q.; Kinch, L.N.; Schaeffer, R.D.; et al. Accurate prediction of protein structures and interactions using a three-track neural network. *Science* **2021**, *373*, 871–876. [[CrossRef](#)]
24. Hilario, E.; da Silva, S.L.F.; Ramos, C.H.I.; Bertolini, M.C. Effects of cardiomyopathic mutations on the biochemical and biophysical properties of the human α -tropomyosin. *JBIC J. Biol. Inorg. Chem.* **2004**, *271*, 4132–4140. [[CrossRef](#)]
25. Rosli, N.E.; Ali, M.S.M.; Kamarudin, N.H.A.; Masomian, M.; Latip, W.; Saadon, S.; Rahman, R.N.Z.R.A. Structure Prediction and Characterization of Thermostable Aldehyde Dehydrogenase from Newly Isolated *Anoxybacillus geothermalis* Strain D9. *Microorganisms* **2022**, *10*, 1444. [[CrossRef](#)]
26. Jesus, C.N.; Evans, R.; Forth, J.; Estarellas, C.; Gervasio, F.L.; Battaglia, G. Amphiphilic Histidine-Based Oligopeptides Exhibit pH-Reversible Fibril Formation. *ACS Macro Lett.* **2021**, *10*, 984–989. [[CrossRef](#)]
27. Regis, W.C.; Fattori, J.; Santoro, M.M.; Jamin, M.; Ramos, C.H. On the difference in stability between horse and sperm whale myoglobins. *Arch. Biochem. Biophys.* **2005**, *436*, 168–177. [[CrossRef](#)]
28. Opassi, G.; Nordström, H.; Lundin, A.; Napolitano, V.; Magari, F.; Dzuz, T.; Klebe, G.; Danielson, U.H. Establishing *Trypanosoma cruzi* farnesyl pyrophosphate synthase as a viable target for biosensor driven fragment-based lead discovery. *Protein Sci.* **2020**, *29*, 977–989. [[CrossRef](#)]
29. dos Santos, R.V.; Grillo, G.; Fonseca, H.; Stanisic, D.; Tasic, L. Hesperitin as an inhibitor of the snake venom serine protease from *Bothrops jararaca*. *Toxicon* **2021**, *198*, 64–72. [[CrossRef](#)]
30. Ruzza, P.; Honisch, C.; Hussain, R.; Siligardi, G. Free Radical Generation in Far-UV Synchrotron Radiation Circular Dichroism Assays—Protein and Buffer Composition Contribution. *Int. J. Mol. Sci.* **2021**, *22*, 11325. [[CrossRef](#)]
31. Spöttel, J.; Brockelt, J.; Falke, S.; Rohn, S. Characterization of Conjugates between α -Lactalbumin and Benzyl Isothiocyanate—Effects on Molecular Structure and Proteolytic Stability. *Molecules* **2021**, *26*, 6247. [[CrossRef](#)]
32. Shiratori, T.; Goto, S.; Sakaguchi, T.; Kasai, T.; Otsuka, Y.; Higashi, K.; Makino, K.; Takahashi, H.; Komatsu, K. Singular value decomposition analysis of the secondary structure features contributing to the circular dichroism spectra of model proteins. *Biochem. Biophys. Rep.* **2021**, *28*, 101153. [[CrossRef](#)]
33. Rajkovic, A.; Kanchugal, S.; Abdurakhmanov, E.; Howard, R.; Wärmländer, S.; Erwin, J.; Saldaña, H.A.B.; Gräslund, A.; Danielson, H.; Flores, S.C. Amino acid substitutions in human growth hormone affect secondary structure and receptor binding. *PLoS ONE* **2023**, *18*, e0282741. [[CrossRef](#)]
34. Ramos, C.H.I.; Weisbuch, S.; Jamin, M. Diffusive Motions Control the Folding and Unfolding Kinetics of the Apomyoglobin pH 4 Molten Globule Intermediate. *Biochemistry* **2007**, *46*, 4379–4389. [[CrossRef](#)]
35. Menard, L.M.; Wood, N.B.; Vigoreaux, J.O. Secondary Structure of the Novel Myosin Binding Domain WYR and Implications within Myosin Structure. *Biology* **2021**, *10*, 603. [[CrossRef](#)] [[PubMed](#)]
36. Stifter, S.A.; Matthews, A.Y.; Mangan, N.E.; Fung, K.Y.; Drew, A.; Tate, M.D.; da Costa, T.P.S.; Hampsey, D.; Mayall, J.; Hansbro, P.M.; et al. Defining the distinct, intrinsic properties of the novel type I interferon, IFN ϵ . *J. Biol. Chem.* **2018**, *293*, 3168–3179. [[CrossRef](#)] [[PubMed](#)]

37. Ishak, S.N.H.; Kamarudin, N.H.A.; Ali, M.S.M.; Leow, A.T.C.; Rahman, R.N.Z.R.A. Ion-Pair Interaction and Hydrogen Bonds as Main Features of Protein Thermostability in Mutated T1 Recombinant Lipase Originating from *Geobacillus zalihae*. *Molecules* **2020**, *25*, 3430. [[CrossRef](#)] [[PubMed](#)]
38. Nefedova, V.V.; Yampolskaya, D.S.; Kleymenov, S.Y.; Chebotareva, N.A.; Matyushenko, A.M.; Levitsky, D.I. Effect of Neurodegenerative Mutations in the NEFL Gene on Thermal Denaturation of the Neurofilament Light Chain Protein. *Biochemistry* **2023**, *88*, 610–620. [[CrossRef](#)] [[PubMed](#)]
39. Sprecher, C.A.; Baase, W.A.; Johnson, W.C. Conformation and circular dichroism of DNA. *Biopolymers* **1979**, *18*, 1009–1019. [[CrossRef](#)] [[PubMed](#)]
40. Marqusee, S.; Baldwin, R.L. Helix stabilization by Glu...Lys+ salt bridges in short peptides of de novo design. *Proc. Natl. Acad. Sci. USA* **1987**, *84*, 8898–8902. [[CrossRef](#)] [[PubMed](#)]
41. Morrisett, J.D.; David, J.S.K.; Pownall, H.J.; Gotto, A.M. Interaction of an apolipoprotein (apoLP-alanine) with phosphatidylcholine. *Biochemistry* **1973**, *12*, 1290–1299. [[CrossRef](#)]
42. Chen, Y.-H.; Yang, J.T.; Chau, K.H. Determination of the helix and β form of proteins in aqueous solution by circular dichroism. *Biochemistry* **1974**, *13*, 3350–3359. [[CrossRef](#)]
43. Greenfield, N.J.; Fasman, G.D. Computed circular dichroism spectra for the evaluation of protein conformation. *Biochemistry* **1969**, *8*, 4108–4116. [[CrossRef](#)] [[PubMed](#)]
44. Miles, A.J.; Ramalli, S.G.; Wallace, B.A. DichroWeb, a website for calculating protein secondary structure from circular dichroism spectroscopic data. *Protein Sci.* **2021**, *31*, 37–46. [[CrossRef](#)]
45. Louis-Jeune, C.; Andrade-Navarro, M.A.; Perez-Iratxeta, C. Prediction of protein secondary structure from circular dichroism using theoretically derived spectra. *Proteins: Struct. Funct. Bioinform.* **2011**, *80*, 374–381. [[CrossRef](#)]
46. Nagy, G.; Igaev, M.; Jones, N.C.; Hoffmann, S.V.; Grubmüller, H. SESCA: Predicting Circular Dichroism Spectra from Protein Molecular Structures. *J. Chem. Theory Comput.* **2019**, *15*, 5087–5102. [[CrossRef](#)]
47. Drew, E.D.; Janes, R.W. PDBMD2CD: Providing predicted protein circular dichroism spectra from multiple molecular dynamics-generated protein structures. *Nucleic Acids Res.* **2020**, *48*, W17–W24. [[CrossRef](#)]
48. Brookes, E.; Rocco, M. A database of calculated solution parameters for the AlphaFold predicted protein structures. *Sci. Rep.* **2022**, *12*, 7349. [[CrossRef](#)]
49. Gill, S.C.; von Hippel, P.H. Calculation of protein extinction coefficients from amino acid sequence data. *Anal. Biochem.* **1989**, *182*, 319–326. [[CrossRef](#)]
50. Pace, C.N.; Vajdos, F.; Fee, L.; Grimsley, G.; Gray, T. How to measure and predict the molar absorption coefficient of a protein. *Protein Sci.* **1995**, *4*, 2411–2423. [[CrossRef](#)]
51. Edelhoch, H. Spectroscopic Determination of Tryptophan and Tyrosine in Proteins. *Biochemistry* **1967**, *6*, 1948–1954. [[CrossRef](#)]
52. Schmid, F. Optical spectroscopy to characterize protein conformation and conformational changes. In *Protein Structure: A Practical Approach*; Creighton, T.E., Ed.; Oxford University Press: New York, NY, USA, 1997; pp. 261–297.
53. Kelly, S.M.; Jess, T.J.; Price, N.C. How to study proteins by circular dichroism. *Biochim. Biophys. Acta Proteins Proteom.* **2005**, *1751*, 119–139. [[CrossRef](#)]
54. Greenfield, N.J. Using circular dichroism spectra to estimate protein secondary structure. *Nat. Protoc.* **2006**, *1*, 2876–2890. [[CrossRef](#)]
55. Corrêa, D.H.A.; Ramos, C.H.I. The use of circular dichroism spectroscopy to study protein folding, form and function. *Afr. J. Biochem. Res.* **2009**, *3*, 164–173.
56. Buck, M. Trifluoroethanol and colleagues: Cosolvents come of age. Recent studies with peptides and proteins. *Q. Rev. Biophys.* **1998**, *31*, 297–355. [[CrossRef](#)]
57. Mares-Guia, T.R.; Maigret, B.; Martins, N.F.; Maia, A.L.T.; Vilela, L.; Ramos, C.H.I.; Neto, L.J.; Juliano, M.A.; dos Mares-Guia, M.L.; Santoro, M.M. Molecular dynamics and circular dichroism studies of human and rat C-peptides. *J. Mol. Graph. Model.* **2006**, *25*, 532–542. [[CrossRef](#)]
58. Timasheff, S.N. The Control of Protein Stability and Association by Weak Interactions with Water: How Do Solvents Affect These Processes? *Annu. Rev. Biophys. Biomol. Struct.* **1993**, *22*, 67–97. [[CrossRef](#)]
59. Ramos, C.H.I. Mapping Subdomains in the C-terminal Region of Troponin I Involved in Its Binding to Troponin C and to Thin Filament. *J. Biol. Chem.* **1999**, *274*, 18189–18195. [[CrossRef](#)]
60. Ramos, C.H.; Ferreira, S.T. Protein Folding, Misfolding and Aggregation: Evolving Concepts and Conformational Diseases. *Protein Pept. Lett.* **2005**, *12*, 213–222. [[CrossRef](#)]
61. Ramos, C.H.; Lima, M.V.; Silva, S.L.; Borin, P.F.; Régis, W.C.; Santoro, M.M. Stability and folding studies of the N-domain of troponin C. Evidence for the formation of an intermediate. *Arch. Biochem. Biophys.* **2004**, *427*, 135–142. [[CrossRef](#)]
62. Benjwal, S.; Verma, S.; Röhm, K.-H.; Gursky, O. Monitoring protein aggregation during thermal unfolding in circular dichroism experiments. *Protein Sci.* **2006**, *15*, 635–639. [[CrossRef](#)]
63. Miles, A.J.; Wallace, B.A. Synchrotron radiation circular dichroism spectroscopy of proteins and applications in structural and functional genomics. *Chem. Soc. Rev.* **2005**, *35*, 39–51. [[CrossRef](#)]
64. Wallace, B.; Janes, R.W. Synchrotron radiation circular dichroism (SRCD) spectroscopy: An enhanced method for examining protein conformations and protein interactions. *Biochem. Soc. Trans.* **2010**, *38*, 861–873. [[CrossRef](#)] [[PubMed](#)]

65. Kumagai, P.S.; Araujo, A.P.U.; Lopes, J.L.S. Going deep into protein secondary structure with synchrotron radiation circular dichroism spectroscopy. *Biophys. Rev.* **2017**, *9*, 517–527. [[CrossRef](#)] [[PubMed](#)]
66. Karlsson, E.; Andersson, E.; Jones, N.C.; Hoffmann, S.V.; Jemth, P.; Kjaergaard, M. Coupled Binding and Helix Formation Monitored by Synchrotron-Radiation Circular Dichroism. *Biophys. J.* **2019**, *117*, 729–742. [[CrossRef](#)]
67. Makumire, S.; Zininga, T.; Vahokoski, J.; Kursula, I.; Shonhai, A. Biophysical analysis of Plasmodium falciparum Hsp70-Hsp90 organising protein (PfHop) reveals a monomer that is characterised by folded segments connected by flexible linkers. *PLoS ONE* **2020**, *15*, e0226657. [[CrossRef](#)] [[PubMed](#)]
68. Almeida, A.V.; Jacinto, J.P.; Guerra, J.P.L.; Vieira, B.J.C.; Waerenborgh, J.C.; Jones, N.C.; Hoffmann, S.V.; Pereira, A.S.; Tavares, P. Structural features and stability of apo- and holo-forms of a simple iron–sulfur protein. *Eur. Biophys. J.* **2021**, *50*, 561–570. [[CrossRef](#)] [[PubMed](#)]
69. Théron, L.; Bonifacie, A.; Delabre, J.; Sayd, T.; Aubry, L.; Gatellier, P.; Ravel, C.; Chambon, C.; Astruc, T.; Rouel, J.; et al. Investigation by Synchrotron Radiation Circular Dichroism of the Secondary Structure Evolution of Pepsin under Oxidative Environment. *Foods* **2021**, *10*, 998. [[CrossRef](#)]
70. Buckley, A.; Warren, J.; Hussain, R.; Smith, R. Synchrotron radiation circular dichroism spectroscopy reveals that gold and silver nanoparticles modify the secondary structure of a lung surfactant protein B analogue. *Nanoscale* **2023**, *15*, 4591–4603. [[CrossRef](#)] [[PubMed](#)]
71. Wien, F.; Kubiak, K.; Turbant, F.; Mosca, K.; Węgrzyn, G.; Arluison, V. Synchrotron Radiation Circular Dichroism, a New Tool to Probe Interactions between Nucleic Acids Involved in the Control of ColE1-Type Plasmid Replication. *Appl. Sci.* **2022**, *12*, 2639. [[CrossRef](#)]
72. Cappannini, A.; Mosca, K.; Mukherjee, S.; Moafinejad, S.N.; Sinden, R.R.; Arluison, V.; Bujnicki, J.; Wien, F. NACDDB: Nucleic Acid Circular Dichroism Database. *Nucleic Acids Res.* **2022**, *51*, D226–D231. [[CrossRef](#)]
73. Harada, T.; Moriyama, H. Solid-State Circular Dichroism Spectroscopy. In *Encyclopedia of Polymer Science and Technology*, 3rd ed.; Mark, H.F., Ed.; John Wiley & Sons: Hoboken, NJ, USA, 2013; pp. 1–29.
74. Castiglioni, E.; Biscarini, P.; Abbate, S. Experimental aspects of solid state circular dichroism. *Chirality* **2009**, *21*, E28–E36. [[CrossRef](#)]
75. Sanchez-Rexach, E.; Smith, P.T.; Gomez-Lopez, A.; Fernandez, M.; Cortajarena, A.L.; Sardon, H.; Nelson, A. 3D-Printed Bioplastics with Shape-Memory Behavior Based on Native Bovine Serum Albumin. *ACS Appl. Mater. Interfaces* **2021**, *13*, 19193–19199. [[CrossRef](#)]
76. Kuroda, R.; Harada, T.; Shindo, Y. A solid-state dedicated circular dichroism spectrophotometer: Development and application. *Rev. Sci. Instrum.* **2001**, *72*, 3802–3810. [[CrossRef](#)]
77. Sunde, M.; Blake, C.C.F. From the globular to the fibrous state: Protein structure and structural conversion in amyloid formation. *Q. Rev. Biophys.* **1998**, *31*, 1–39. [[CrossRef](#)]
78. Hu, H.Y.; Li, Q.; Cheng, H.C.; Du, H.N. β -sheet structure formation of proteins in solid state as revealed by circular dichroism spectroscopy. *Biopolym. Orig. Res. Biomol.* **2001**, *62*, 15–21. [[CrossRef](#)]
79. Hu, H.-Y.; Jiang, L.-L.; Hong, J.-Y. Study of Protein Amyloid-Like Aggregates by Solid-State Circular Dichroism Spectroscopy. *Curr. Protein Pept. Sci.* **2016**, *18*, 100–103. [[CrossRef](#)]
80. Brown, C.P.; Hughes, M.D.G.; Mahmoudi, N.; Brockwell, D.J.; Coletta, P.L.; Peyman, S.A.; Evans, S.D.; Dougan, L. Structural and mechanical properties of folded protein hydrogels with embedded microbubbles. *Biomater. Sci.* **2023**, *11*, 2726–2737. [[CrossRef](#)]
81. Hughes, M.D.G.; Cussons, S.; Mahmoudi, N.; Brockwell, D.J.; Dougan, L. Single molecule protein stabilisation translates to macromolecular mechanics of a protein network. *Soft Matter* **2020**, *16*, 6389–6399. [[CrossRef](#)]
82. Adams, Z.C.; Olson, E.J.; Lopez-Silva, T.L.; Lian, Z.; Kim, A.Y.; Holcomb, M.; Zimmermann, J.; Adhikary, R.; Dawson, P.E. Direct observation of peptide hydrogel self-assembly. *Chem. Sci.* **2022**, *13*, 10020–10028. [[CrossRef](#)]
83. Baumruk, V.; Keiderling, T.A. Vibrational circular dichroism of proteins in water solution. *J. Am. Chem. Soc.* **1993**, *115*, 6939–6942. [[CrossRef](#)]
84. Yang, G.; Xu, Y. Vibrational Circular Dichroism Spectroscopy of Chiral Molecules. In *Electronic and Magnetic Properties of Chiral Molecules and Supramolecular Architectures*; Topics in Current Chemistry; Naaman, R., Beratan, D., Waldeck, D., Eds.; Springer: Berlin/Heidelberg, Germany, 2010; Volume 298, pp. 189–236. [[CrossRef](#)]
85. Li, Z.; Hirst, J.D. Quantitative first principles calculations of protein circular dichroism in the near-ultraviolet. *Chem. Sci.* **2017**, *8*, 4318–4333. [[CrossRef](#)]
86. Kurouski, D. Advances of Vibrational Circular Dichroism (VCD) in bioanalytical chemistry. A review. *Anal. Chim. Acta* **2017**, *990*, 54–66. [[CrossRef](#)]
87. Xu, C.; Ren, Z.; Zhou, H.; Zhou, J.; Ho, C.P.; Wang, N.; Lee, C. Expanding chiral metamaterials for retrieving fingerprints via vibrational circular dichroism. *Light Sci. Appl.* **2023**, *12*, 154. [[CrossRef](#)]
88. Kessler, J.; Andrushchenko, V.; Kapitán, J.; Bouř, P. Insight into vibrational circular dichroism of proteins by density functional modeling. *Phys. Chem. Chem. Phys.* **2018**, *20*, 4926–4935. [[CrossRef](#)]
89. Litwińczuk, A.; Ryu, S.R.; Nafie, L.A.; Lee, J.W.; Kim, H.I.; Jung, Y.M.; Czarnik-Matusiewicz, B. The transition from the native to the acid-state characterized by multi-spectroscopy approach: Study for the holo-form of bovine α -lactalbumin. *Biochim. Biophys. Acta (BBA)—Proteins Proteom.* **2014**, *1844*, 593–606. [[CrossRef](#)]

90. Rudd, T.R.; Nichols, R.J.; Yates, E.A. Selective Detection of Protein Secondary Structural Changes in Solution Protein–Polysaccharide Complexes Using Vibrational Circular Dichroism (VCD). *J. Am. Chem. Soc.* **2008**, *130*, 2138–2139. [[CrossRef](#)]
91. Kurouski, D.; Lu, X.; Popova, L.; Wan, W.; Shanmugasundaram, M.; Stubbs, G.; Dukor, R.K.; Lednev, I.K.; Nafie, L.A. Is Supramolecular Filament Chirality the Underlying Cause of Major Morphology Differences in Amyloid Fibrils? *J. Am. Chem. Soc.* **2014**, *136*, 2302–2312. [[CrossRef](#)]
92. Pazderková, M.; Pazderka, T.; Shanmugasundaram, M.; Dukor, R.K.; Lednev, I.K.; Nafie, L.A. Origin of enhanced VCD in amyloid fibril spectra: Effect of deuteration and pH. *Chirality* **2017**, *29*, 469–475. [[CrossRef](#)]
93. Keiderling, T.A. Structure of Condensed Phase Peptides: Insights from Vibrational Circular Dichroism and Raman Optical Activity Techniques. *Chem. Rev.* **2020**, *120*, 3381–3419. [[CrossRef](#)]

Disclaimer/Publisher’s Note: The statements, opinions and data contained in all publications are solely those of the individual author(s) and contributor(s) and not of MDPI and/or the editor(s). MDPI and/or the editor(s) disclaim responsibility for any injury to people or property resulting from any ideas, methods, instructions or products referred to in the content.